CONF-750360--2

A CRACKED PELLET GAP CONDUCTANCE MODEL - COMPARISON OF FRAP-S CALCULATIONS WITH MEASURED FUEL CENTERLINE TEMPERATURES

by

P. E. MacDonald and J. M. Broughton

AEROJET NUCLEAR COMPANY

March 1975

ABSTRACT

Fuel pellets crack extensively upon irradiation due both to thermal stresses induced by power changes and at high burnup, to accumulation of gaseous fission products at grain boundaries. Therefore, the distance between the fuel and cladding will be circumferentially nonuniform; varying between that calculated for intact operating fuel pellets and essentially zero (fuel segments in contact with the cladding wall). A model for calculation of temperatures in cracked pellets is proposed wherein the effective fuel to cladding gap conductance is calculated by taking a zero pressure contact conductance in series with an annular gap conductance. Comparisons of predicted and measured fuel centerline temperatures at beginning of life and at extended burnup are presented in support of the model.

CONTENTS

PREPARED FOR THE U. S. ATOMIC ENERGY COMMISSION
IDAHO OPERATIONS OFFICE
UNDER CONTRACT NO. AT(10-1)-1375

I. INTRODUCTION

Understanding the performance of light-water reactor fuel under normal and accident conditions is a major objective of the Nuclear Regulatory Commission reactor safety research program. An extensive program has been defined - centered upon out-of-pile and inpile experiments and analysis of such experiments -with the goal of verifying analytical codes. These codes, when verified, will be capable of predicting fuel transient performance for a broad spectrum of accident types and a wide range of conditions, at any time during the normal useful life of a fuel rod.

Analysis of fuel behavior during an accident depends on knowledge of fuel rod conditions during normal (steady state) operation. Especially important are the temperature distributions of the fuel pellets, the geometry of fuel rod components, the internal gas pressure and composition, the amount of restructuring and cracking of the pellets, and the mechanical strains and irradiation damage in the cladding. All of these parameters are affected by the rod design variables at beginning of life, and subsequently, by the power history and the degree of burnup. A computer code (FRAP-S) to predict this behavior is under development at Aerojet Nuclear Company. This paper describes a cracked pellet gap conductance model developed for use in this code. Comparisons of model predictions using the proposed cracked pellet model and the Ross and Stoute model with fuel centerline temperature data are presented.

Fuel pellets crack extensively upon irradiation due both to thermal stresses induced by power changes and at high burnup, to accumulation of gaseous fission products at grain boundaries. Therefore, the distance between the fuel and cladding will be circumferentially nonuniform; varying between that calculated for intact operating fuel rods and essentially zero (fuel segments lying against

the cladding wall). Since uranium dioxide pellets primarily tend to crack radially, the pellet thermal conductivity will be only slightly influenced by this phenomenon. However, the fuel-to-cladding gap thermal conductance will be strongly increased and will generally correspond to a value reflecting both contact and open gap conductance.

Efforts to calculate fuel temperatures for rods with large hot gaps based on conductance across an annular gap between the cladding and the fuel using the Ross and Stoute model [1, 2] in FRAP-S give poor agreement with available inpile high burnup temperature measurements. Calculated fuel temperatures are much higher than observed, and the calculated effect of fill-gas conductivity is greater than that measured. This disagreement between predictions and measurements is not surprising, because pellet cracking in effect moves the gap thermal resistance towards the center of the pellet and replaces, to a certain extent, gap gas conduction with contact conduction. Calculated fuel temperatures using the cracked pellet gap conductance model in FRAP-S compare well with data throughout burnup.

II ANALYTICAL MODEL

FRAP-S calculates the interrelated effects of fuel and cladding temperatures, rod internal pressure, fuel and cladding elastic and plastic deformation, release of fission product gases, fuel swelling, cladding growth, cladding corrosion, and crud deposition as functions of time and specific power. The fuel rod power history is approximated by a series of steady-state power levels. The length of the rod is divided into a large number of axial segments, each assumed to operate at an average set of conditions over its length. The axial flux (power) shape is input and may be varied as a function of time. Fuel and cladding temperatures, fuel swelling and thermal expansion, cladding growth, cladding stresses and strains, and fission gas releases are calculated separately for each axial segment. The fission gas release and fuel

and cladding deformations are then integrated over the length of the fuel rod and added to previous power step values to obtain the rod internal pressure. This pressure is fed back into the fuel and cladding elastic and plastic deflection calculations in subsequent iterations.

Figure 1 presents a summary of the major interactions dealt with by FRAP-S. Due to the large number of interactions and feedbacks among the thermal conditions and the physical behavior of a fuel pin, several iterative processes are nested in the code calculations. The major iterative loops are:

(1) At each axial increment, the gap and fuel temperatures, the fuel thermal expansion, and the cladding strain are iterated until convergence is obtained.

(2) At each specified time step, the entire rod conditions are recalculated with interations continued until gas release and rod internal pressure are unchanged.

The Mikic [3, 4] theory with modification when the fuel and cladding surfaces are behaving elastically as proposed by Jacobs and Todreas [5] is used in FRAP-S to calculate the gap conductance when the fuel and cladding are in hard contact. If a nominal open hot gap is calculated, a fraction of the fuel pellet is assumed to be in contact with the cladding and an effective fuel-to-cladding gap conductance is calculated as follows:

$$h_{gap} = (1-F)\, h_o + F\, h_c \qquad (1)$$

where

h_{gap} = net gap conductance, W/m^2-K

h_o = open gap conductance, W/m^2-K

h_c = contact gap conductance, W/m^2-K

F = fraction of pellet circumference in contact with the cladding

The open gap conductance is determined from

$$h_o = \frac{k_{mix}}{\Delta r + \delta} \qquad (2)$$

where

k_{mix} = thermal conductivity of gas mixture, W/m-K

Δr = nominal hot radial gap width, m

δ = root mean square of the fuel and the cladding surface roughness. A value of 4.4×10^{-6} meters is normally used.

The zero pressure contact conductance, h_c, is determined directly from the equation for contact gap conductance discussed subsequently. Radiation heat transfer is assumed negligible.

The fraction of pellet circumference in contact with the cladding, F, is assumed to be an inverse power law function of the ratio of the nominal (uncracked) hot radial gap and the hot pellet radius as follows:

$$F = \frac{1}{a_1 \left(\frac{\Delta r \cdot 100}{R_F}\right)^{a_2} + 1.429} + 0.3 \qquad (3)$$

where

R_F = hot radius of the fuel pellet, m

a_1 and a_2 = empirical constants determined from data.

The relationships for a_1 and a_2 as a function of burnup are described by equations 4 and 5, respectively.

$$a_1 = (100 - 98)\, F' \qquad (4)$$

$$a_2 = (4 - 0.5)\, F' \qquad (5)$$

where

$$F' = 1 - \frac{1}{\left(\frac{x - 600}{1000}\right)^4 + 1}$$

x = burnup in MWD/MTU

The fraction of pellet-cladding contact, Equation 3, is plotted in Figure 2 for both beginning and end of life. The burnup relationship, F',

is plotted in Figure 3. Equations 4 and 5 combined with Equation 3 yield a family of curves between the two curves shown in Figure 2. Thus the fraction of the pellet circumference in contact with the cladding is calculated to increase with both decreasing nominal hot radial gas gap and burnup. The asymptotic value of pellet-cladding contact for large gaps, F = 0.3, and the empirical constants a_1 and a_2, were determined empirically by comparison of FRAP-S predictions with the fuel centerline temperature data discussed in Section III.

When the fuel and cladding are in contact, the Mikic theory [3, 4] of thermal contact conductance with modifications as proposed by Jacobs and Todreas [5] for ceramic fuel elements is used. The governing equation for contact conductance is thus

$$h_c = C_1 p^n + \frac{k_{mix}}{\delta} \qquad (6)$$

where:

C_1 = 2.7 for stainless steel cladding and 3.4 for Zircaloy-2 and Zircaloy-4 cladding

p = pellet-cladding contact pressure, psi

n = 1 for $0 \leq P \leq 1000$ psi and 1/2 for $P > 1000$ psi

The value of the exponent, n, is governed by the behavior of the fuel and cladding at the interface of the contact points. An exponent of 1.0 is valid only if the surface peaks of one of the materials are flowing plastically. This type of behavior is consistent with the Ross and Stoute [1] theory of contact conductance. If the contact points of both materials are behaving elastically the correct value for the exponent, n, is approximately 1/2. The experimental results of Fenech and Rohsenow [6] support this value and also indicate that for metal-ceramic pairs the transition pressure from plastic to elastic flow is about 1000 psi. The parameter $\frac{k_{mix}}{\delta}$ in Equation 6 accounts for heat conduction through the gas in the gaps between contact points.

The cladding-fuel gap conductance is also, in part, dependent on the thermal conductivity of the gap gas mixture as shown in Equation 2. The relationship used in FRAP-S for calculating the thermal conductivity of a monatomic gas mixture is based on the work of Brokaw [7], and the thermal conductivity equations of the individual rare gases are based on the correlative work of Ganchi and Saxena [8]. The values published by the Westinghouse Electric Corporation [9] for the thermal conductivity of air, nitrogen, and hydrogen are also included.

The thermal conductivity of the gas mixture is important in determining contact gap conductance as well as open gap conductance in a fuel rod. However, when the ratio of the mean free path of the gas molecules to the characteristic dimension (gap) of the body exceeds about 0.01, the Knudsen domain, normal heat flow formulas become inaccurate. Heat transfer from a solid to a gas in the Knudsen domain is then dependent on an accommodation coefficient which is defined as the ratio of the actual energy interchange to the maximum possible energy interchange between a surface and a gas. Generally, the accommodation coefficient of a heavy gas such as argon or xenon is near unity and is thus neglected. But the change in heat transfer in the Knudsen domain cannot be neglected when the gap is filled with a light gas such as helium. Dean [10] has presented the following factor by which the bulk thermal conductivity of helium should be divided when temperature drops are calculated for the Knudsen domain:

$$f = 1 + \frac{\alpha_1 + \alpha_2 - \alpha_1 \alpha_2}{\alpha_1 \alpha_2} \quad \frac{4}{c_p + c_v} \quad \frac{k}{\mu} \quad \frac{\lambda}{\Delta r} \tag{7}$$

where

α_1 = accommodation coefficient of the fuel

α_2 = accommodation coefficient of the cladding

c_p = constant pressure heat capacity

c_v = constant volume heat capacity

k = gas thermal conductivity

μ = gas viscosity

λ = the mean free path

The mean free path can be written as

$$\lambda = \frac{3\mu}{\rho} \sqrt{\frac{1.22 \times 10^{-2} m}{KT}} \qquad (8)$$

where

m = mass of the molecule

K = Boltzman constant

ρ = density of the gas, $\frac{p}{RT}$

R = ideal gas constant

p = gas pressure

T = gas temperature

If λ and ρ are substituted into Equation 7 and c_p and c_v are assumed not temperature dependent, the Equation 7 can be rewritten as

$$f = 1 + C \frac{k\sqrt{T}}{p\Delta r} \qquad (9)$$

A value for C of approximately 10^{-3} has been used in this study.

III. COMPARISON OF PREDICTIONS WITH EXPERIMENTAL DATA

Fuel centerline temperature comparisons between experimental data and FRAP-S predictions, using both the cracked pellet and the Ross and Stoute [1, 2] gap conductance models, are shown in Figures 4 through 22. Only well characterized rods with known power levels and measured system coolant conditions or cladding temperatures were considered. The following fuel rod conditions are reflected in the data: pellet density (92 - 96% TD), cold diametral gap (2 - 13 mils), and initial internal gas composition (helium and fission gas). Burnup ranged from 0 to about 15,300 MWD/MTU.

The data comparisons are grouped according to initial fill gas and burnup; (1) fission gas filled test rods with little burnup; (2) helium filled rods at beginning of life; and (3) helium filled rods at various burnups. The initial fuel rod conditions for each comparison are summarized on the figure showing that comparison.

Figures 4 through 7 present temperature data from Reference 11 for five capsules. Although the data were taken at relatively low power levels, typical commercial fuel rod dimensions and coolant conditions (except for initial gas composition) are represented. The calculated values obtained using the cracked pellet model are in much better agreement with data from those Reference 11 test rods initially filled with fission gas than are the values calculated using the Ross and Stoute model. Predictions from both models are in reasonable agreement with the data for helium filled rods. These results lend support to the concept that pellet cracking and relocation effectively increase the gap conductance and that a significant proportion of the heat is transferred through mating asperity points rather than by gas gap conduction; even in rods with relatively large initial pellet-to-cladding gaps.

The comparisons of model predictions with data presented in Figures 8 and 9 show centerline temperature data from helium filled rods that were irradiated in the Halden HBWR to about 4200 MWD/MTU[12]. These rods experienced periodic ramps to moderate power levels (approximately 13 kW/ft at the location of temperature measurement) throughout the irradiation period. Figures 8 and 9 show reasonable agreement between the prediction and the measurement for both gap conductance models. In Figure 8 hard fuel-cladding contact is predicted for a major portion of the power ramps (above 4-5 kW/ft). The FRAP-S gap conductance model calculated slightly increased centerline temperatures and changes in temperature with power as compared to the Ross and Stoute model. This result is obtained

because of the assumption in the Mikic model of elastic behavior of the mating asperity points at contact pressures above 1000 psi. Figure 10 compares predictions obtained using both models with measured fuel centerline data reported in Reference 13. Excellent agreement is also shown for these large gap helium filled rods.

Fuel centerline temperature data from the first four days of irradiation, (four power ramps) of the Halden test assembly IFA-226 and model predictions are shown in Figures 11, 12, 13, and 14. The centerline temperature at a given power increased (compared with the preceding power ramp) during the first three power ramps and then stabilized in all four rods. The high power rods, Rods AO and AK, (Figures 12 and 14, respectively) have slightly lower centerline temperatures at power than the lower power rods, Rods AA and AE, (Figures 11 and 13, respectively). This difference in temperature at power would indicate that pellet cracking and relocation resulting from the higher powers experienced during the first ramp of Rods AO and AK resulted in increased gap conductance after temperature stabilization. Rods AA and AO, (Figures 11 and 12, respectively) were fabricated nearly identically and thus the reduction in temperature at power cannot be attributed to the influence of initial dimensions or fuel density. Pellet cracking and relocation effects also appear to negate the difference one would expect among rods of different initial gap width. The centerline temperatures of the large gap rod, Rod AE (Figure 13), are similar to those of the standard rod, Rod AA (Figure 11), after the first power ramp. Figure 15 presents Rod AK centerline fuel temperature measurements taken during both the increasing and decreasing portions of the first and second power ramps. The hysteresis effect at 10 to 14 kW/ft apparently is due to cracked pellet healing at high temperatures, followed by reformation of the pellet-to-cladding gap upon power reduction, followed in turn by the reinitiation of pellet cracking during temperature changes

at low power levels or during the subsequent power ramp. FRAP-S predictions, obtained using both gap conductance models, are in good agreement with these data after the temperatures stabilize (Ramps 3 and 4).

Comparisons of model predictions with IFA-226 fuel centerline temperature data at various burnups to 15,300 MWD/MTU are shown in Figures 16 through 22. These data indicate that burnup effects on pellet cracking and relocation, (and possibly UO_2 thermal conductivity which is not considered) reduce the temperature at a given power in a nonlinear fashion. The effects of burnup do not become noticeable in the experimental data until about 1000 MWD/MTU of burnup and become constant at approximately 10,000 MWD/MTU. Figures 16 through 22 also suggest that, as burnup increases, the Ross and Stoute gap conductance model becomes progressively more conservative. At a burnup of about 15,300 MWD/MTU the Ross and Stoute gap conductance model overpredicts measured fuel centerline temperatures by at least 1000 F. The calculated release of fission product gases degrades the fill gas conductivity at high burnup and, therefore, substantially decreases the Ross and Stoute calculated gap conductance values. FRAP-S predictions obtained using the cracked pellet gap conductance model compare well with the IFA-226 temperature data throughout burnup suggesting that increased pellet cracking and relocation with burnup should compensate for the degradation in gap gas thermal conductivity.

REFERENCES

1. A. M. Ross and R. L. Stoute, Heat Transfer Coefficient Between UO_2 and Zircaloy-2, Report AECL-1552, Chalk River Ontario, (June 1962).

2. C. R. Hann, C. E. Beyer and L. J. Parchen, GAPCON-THERMAL-1: A Computer Program for Calculating the Gap Conductance in Oxide Fuel Pins, Report BNWL-1778 (September 1973).

3. B. B. Mikic and W. M. Rohsenow, Thermal Contact Resistance , DSR 74542-41, Mechanical Engineering Dept., Massachusetts Institute of Technology (1966).

4. H. Fenech and W. M. Rohsenow,"Prediction of Thermal Conductance of Metallic Surfaces in Contact", Paper 62-HT-32, Trans. ASME, Journal of Heat Transfer (March 1963).

5. G. Jacobs and N. Todreas, "Thermal Contact Conductance in Reactor Fuel Elements", Nuclear Science and Engineering, 50 (1973).

6. H. Fenech and W. M. Rohsenow, "Prediction of Thermal Conductance of Metallic Surfaces in Contact", Paper 62-HT-32, Trans. ASME, J. Heat Transfer (March 1973).

7. R. S. Brokaw, Alignment Charts for Transport Properties, Viscosity, Thermal Conductivity and Diffusion Coefficients for Nonpolar Gases and Gas Mixtures at Low Density, Report NASA TR R-81 (1961).

8. J. M. Gandhi and S. C. Saxena, "Correlated Thermal Conductivity Data of Rare Gases and Their Binary Mixtures at Ordinary Pressures," Journal of Chemical and Engineering Data, Vol. 13, No. 3 (1968).

9. Wisconsin Electric Power Company, Fuel Densification, Unit No. 2 - Point Beach Nuclear Plant, Docket No. 50-301 (January 1973).

10. R. A. Dean, Thermal Contact Conductance Between UO_2 and Zircaloy-2, CVNA-127 (1962).

11. I. Cohen, B. Lustman, J. O. Eichenberg, Measurement of the Thermal Conductivity of Metal-Clad Uranium Oxide Rods During Irradiation, WAPD-228, (1960).

12. G. Kjaerheim, and E. Rolstad, In-Pile Determination of UO_2 Thermal Conductivity, Density Effects and Gap Conductance, HPR-80, (December 1967).

13. I. Devold, A Study of the Temperature Distribution in UO_2 Reactor Fuel Elements, Report AE-318, Aktiebolaget Atomenergi, Stockholm, Sweden, (1968).

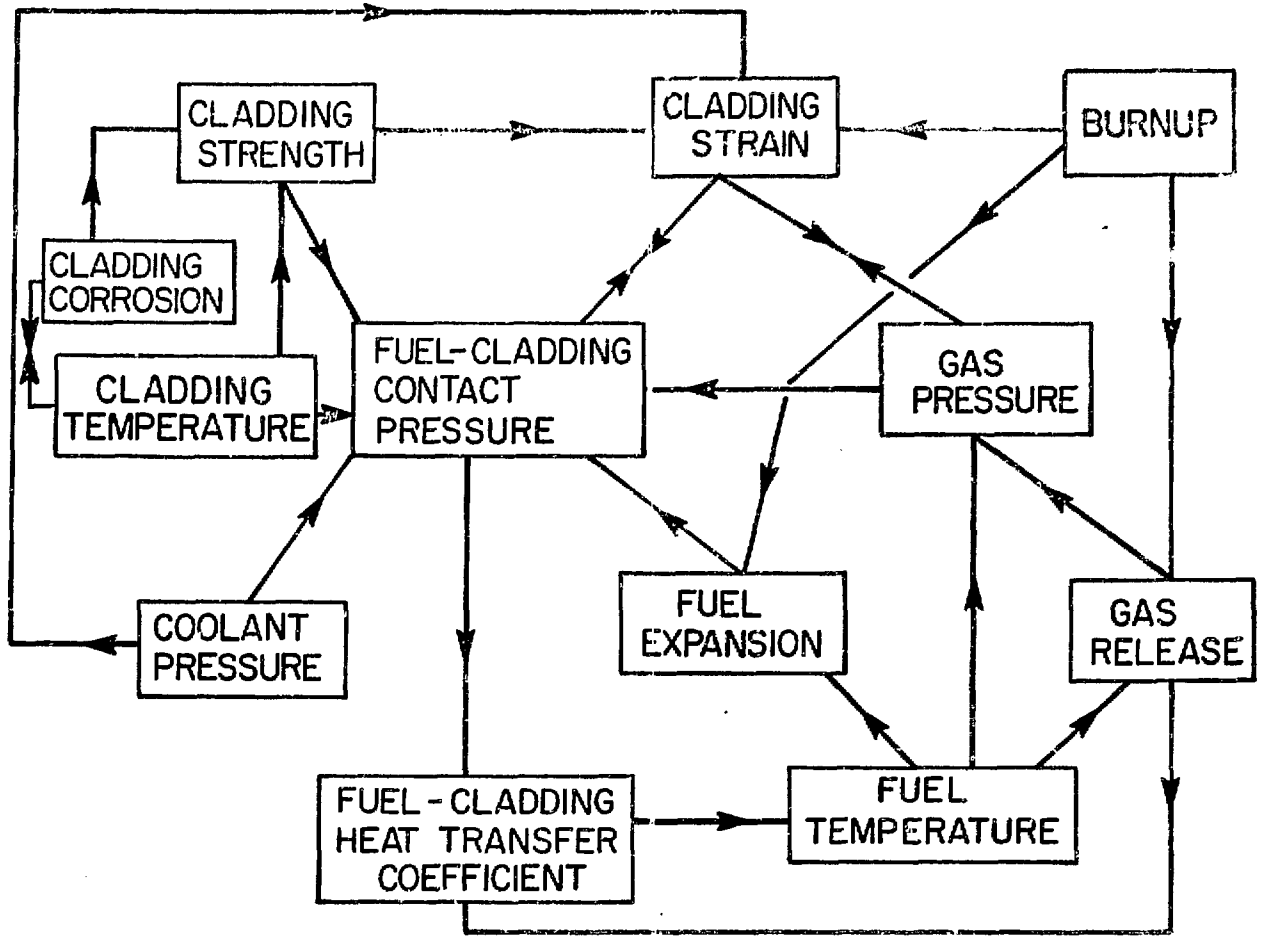

Figure 1 Intermodel Coupling in FRAP-S1

ANC-S-485i

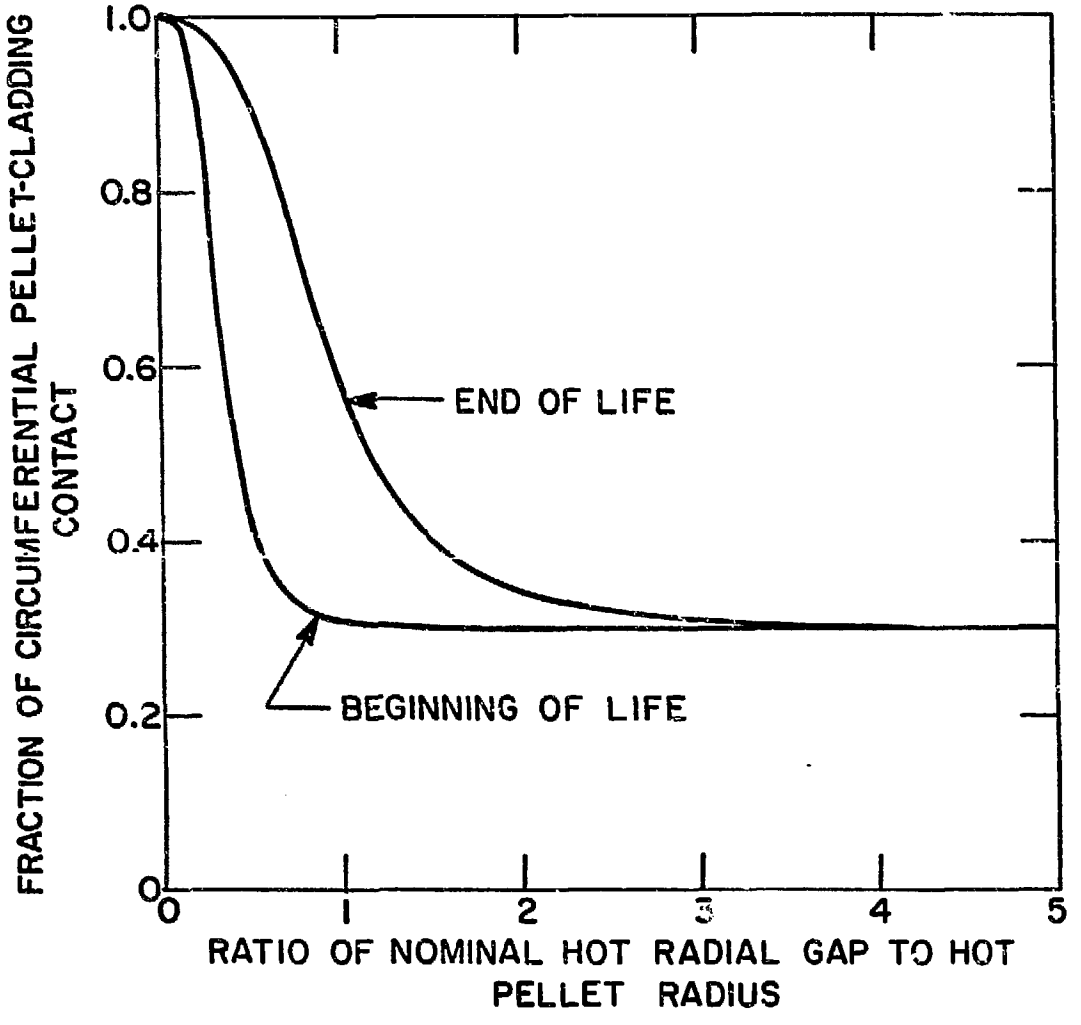

Figure 2 Fraction of pellet circumference in contact with the cladding as a function of the ratio of the nominal hot radial gap to the hot pellet radius.

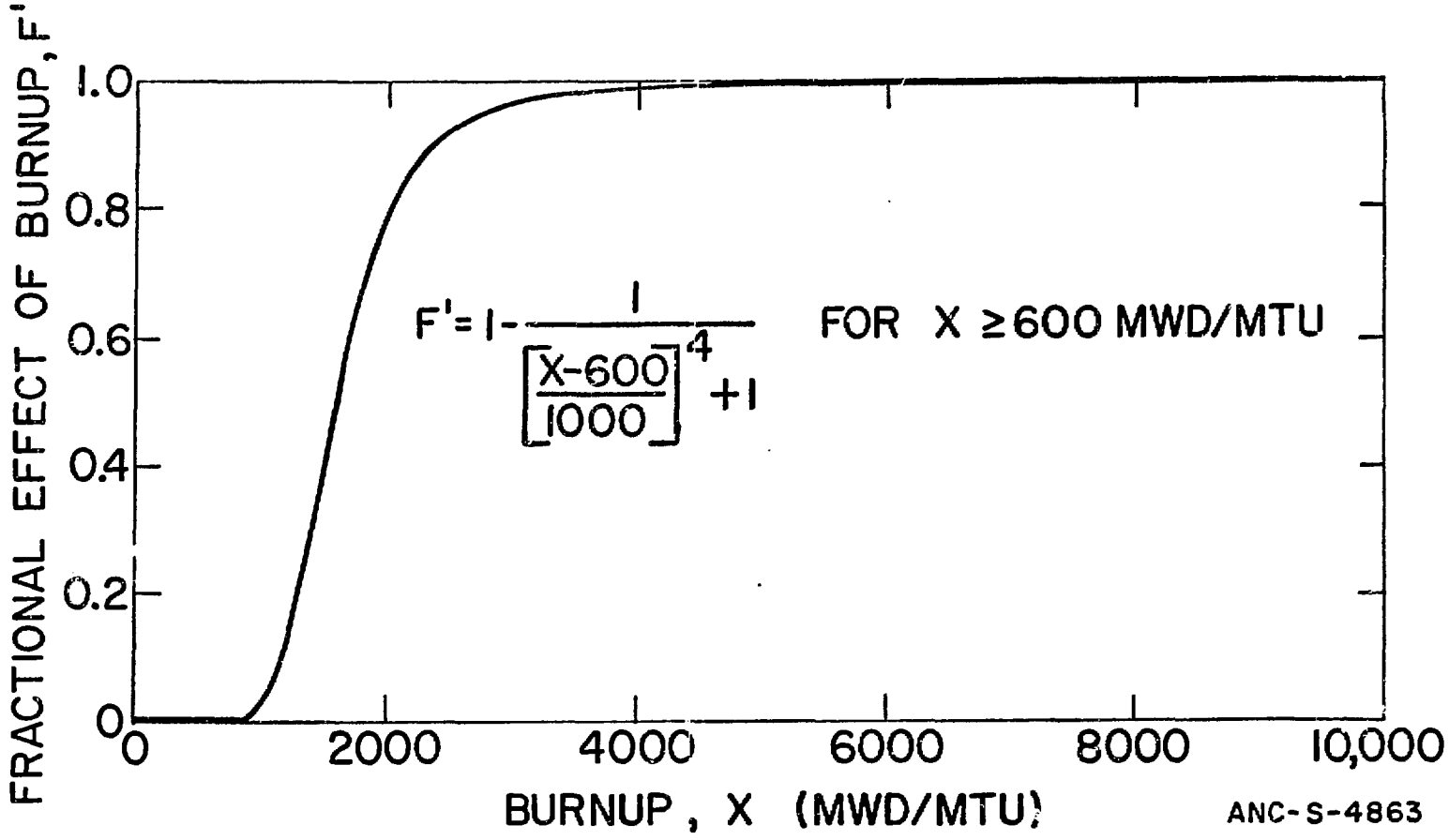

Figure 3 Fractional Effect of burnup as a function of burnup

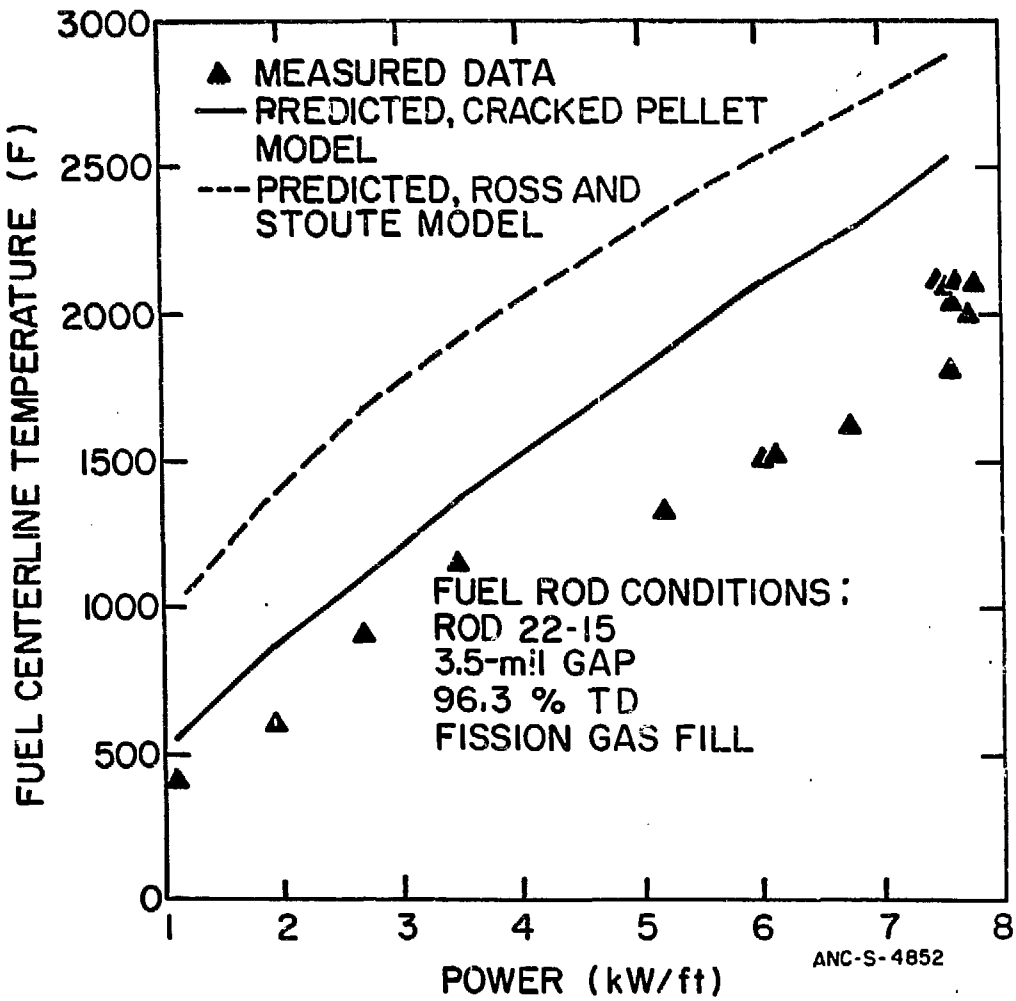

Figure 4 Measured and predicted fuel centerline temperature versus power for Rod 22-15, Reference 11.

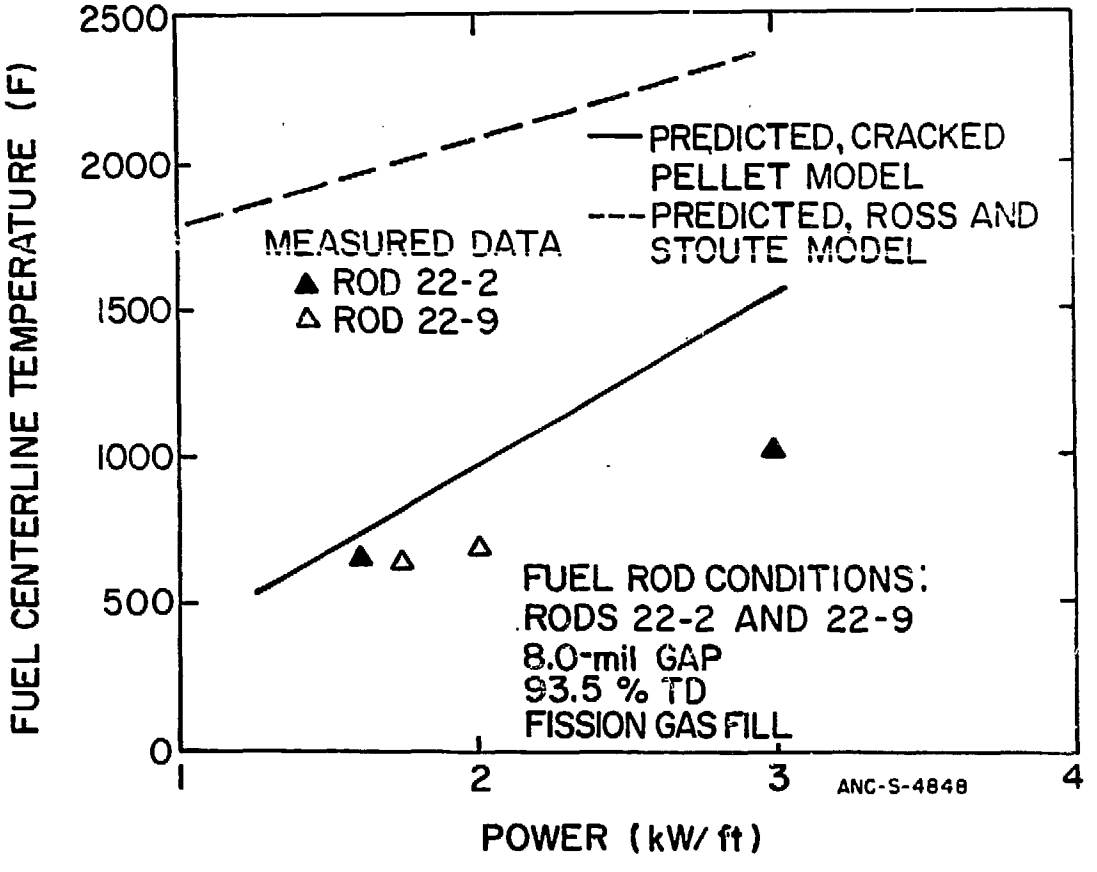

Figure 5 Measured and predicted fuel centerline temperature versus power for Rods 22-2 and 22-9, Reference 11.

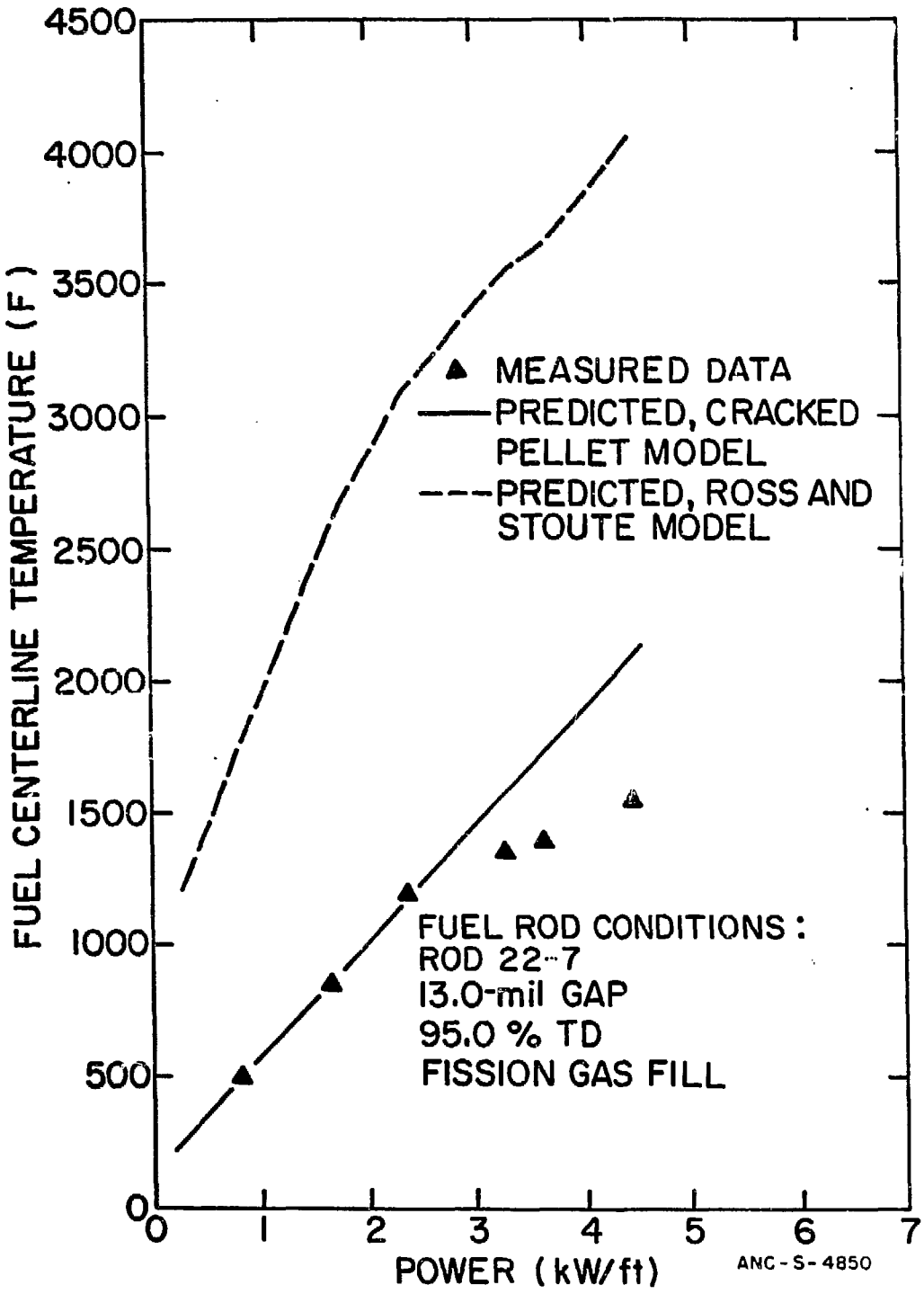

Figure 6 Measured and predicted fuel centerline temperature versus power for Rod 22-7, Reference 11.

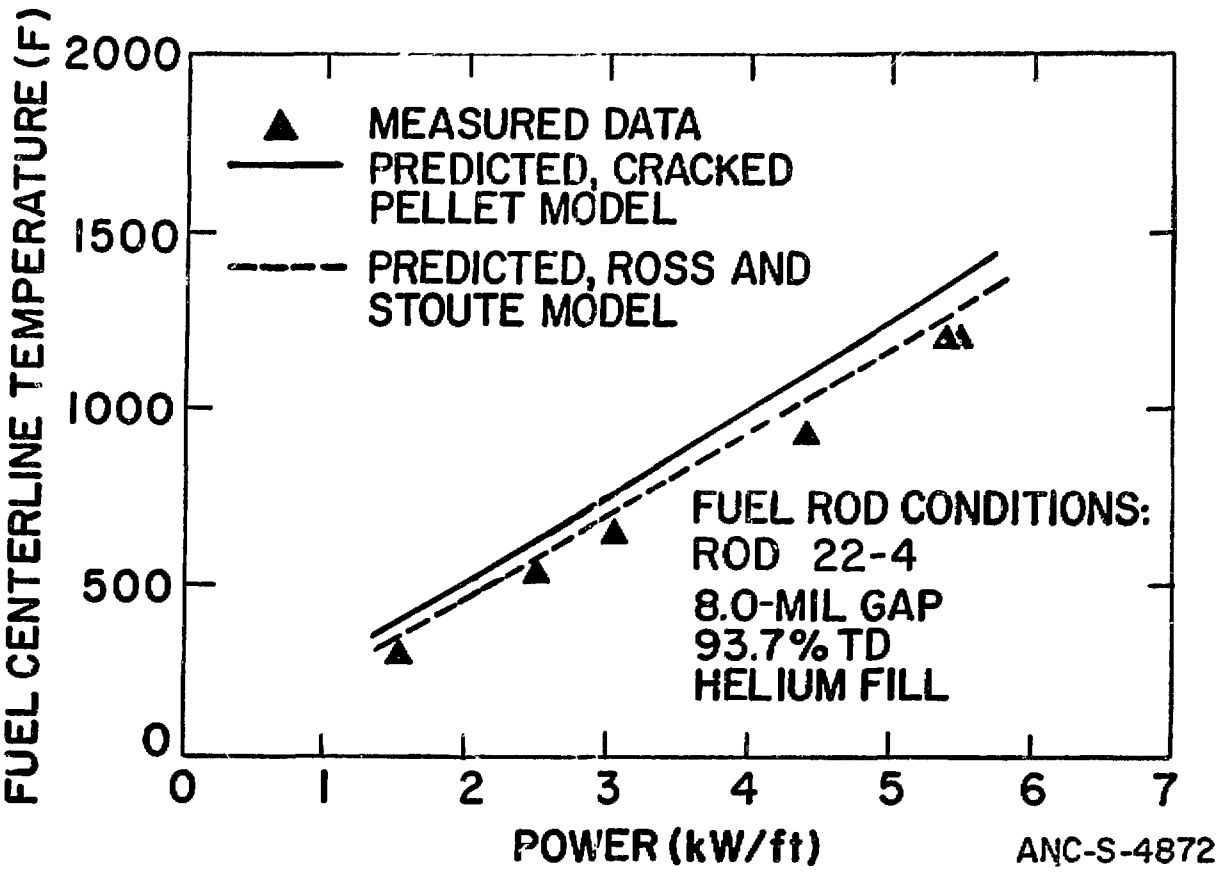

Figure 7 Measured and predicted fuel centerline temperature versus power for Rod 22-4, Reference 11.

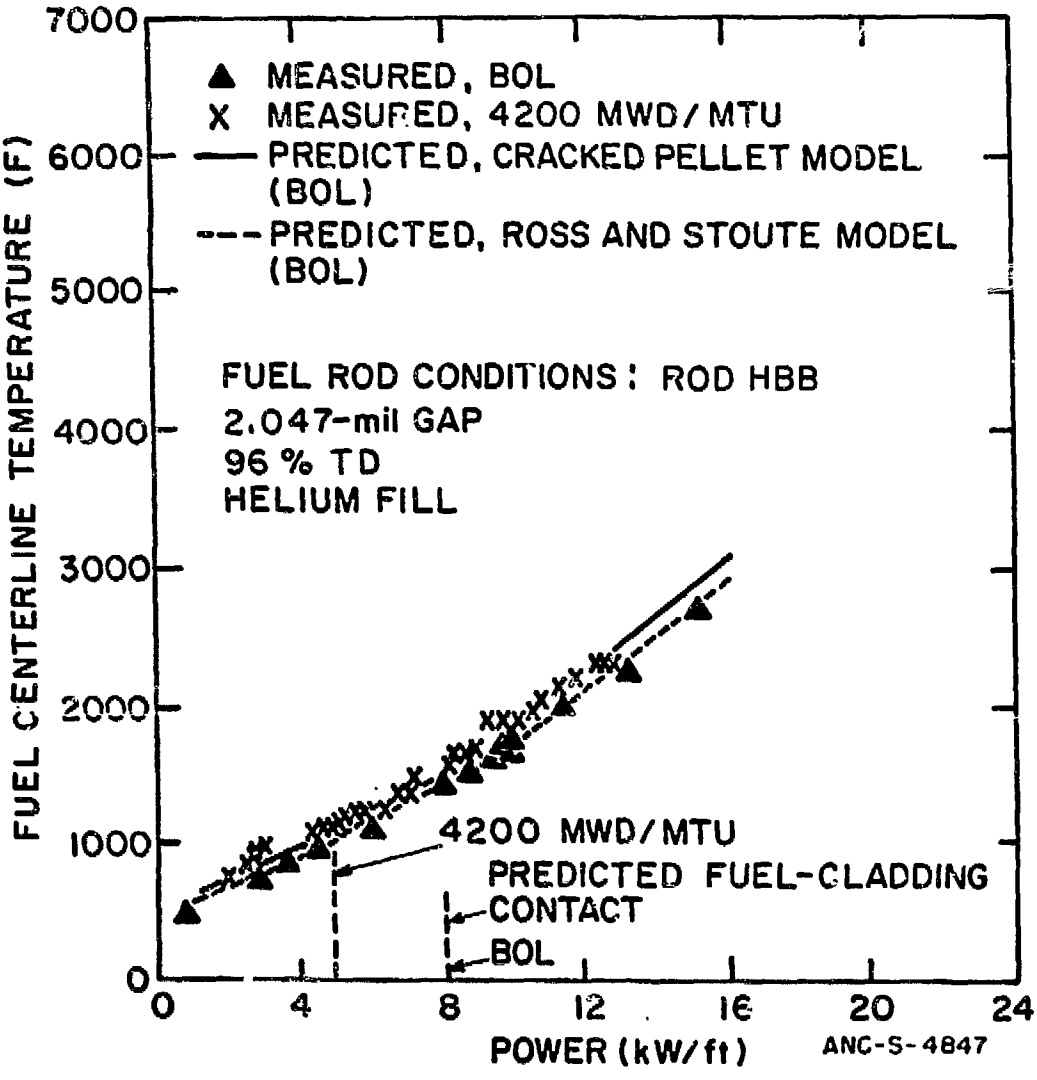

Figure 8 Measured and predicted fuel centerline temperature versus power for Rod HBB, Reference 12.

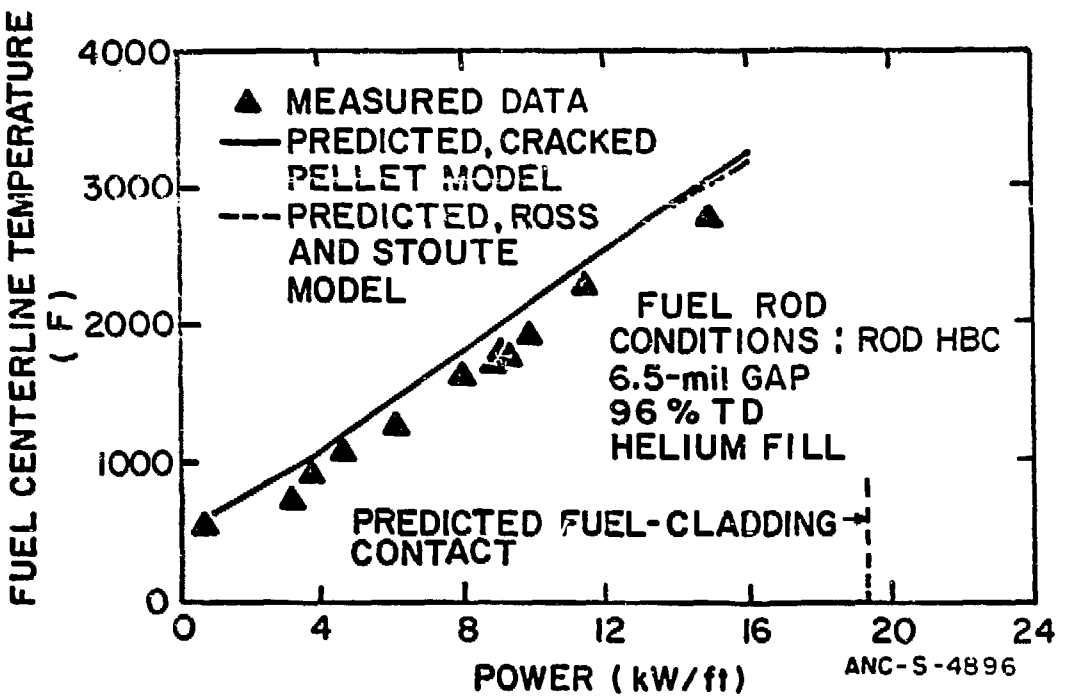

Figure 9 Measured and predicted fuel centerline temperature versus power for Rod HBC, Reference 12.

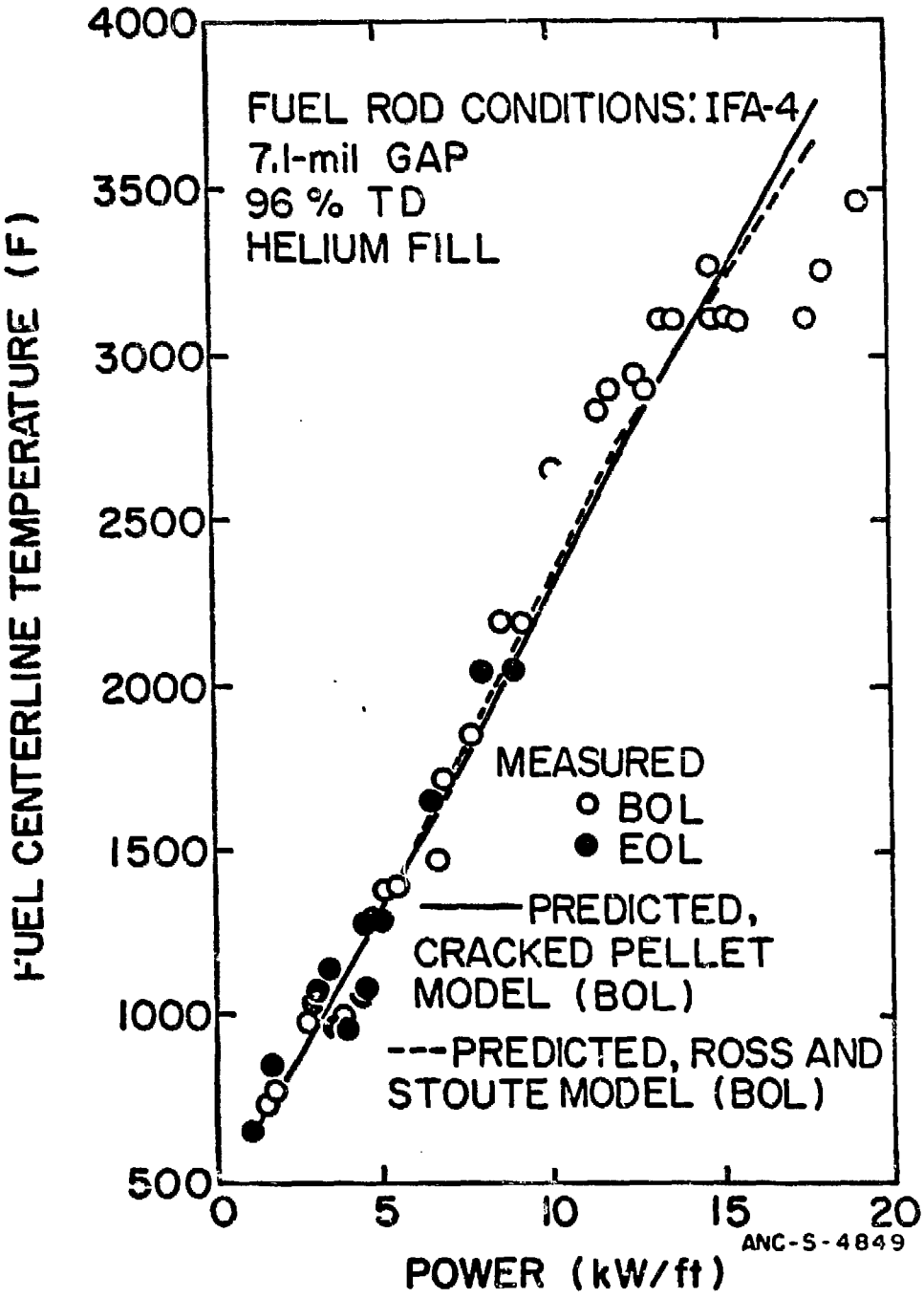

Figure 10 Measured and predicted fuel centerline temperature versus power for the IFA-4 rod, Reference 13.

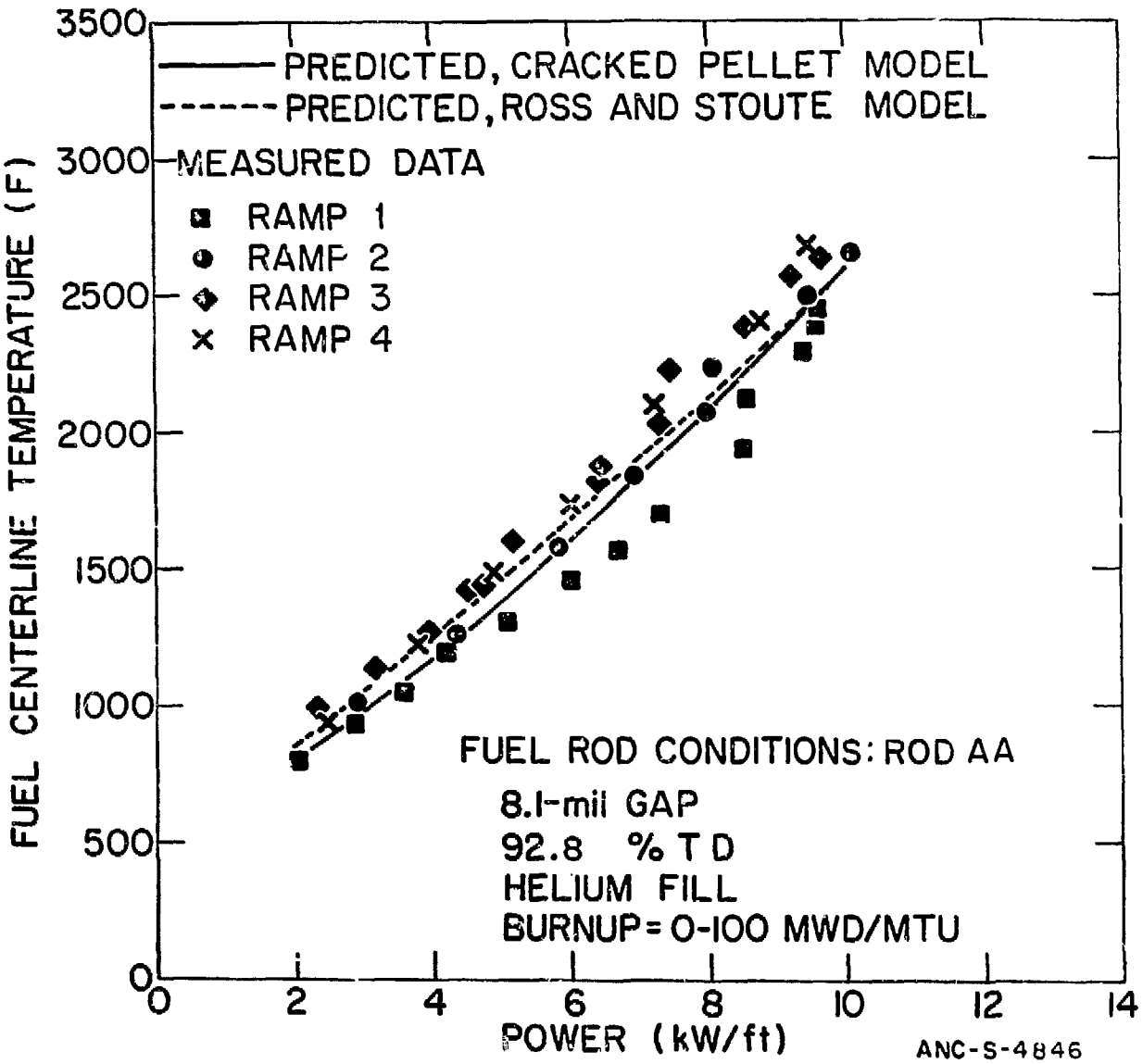

Figure 1: Measured and predicted fuel centerline temperature versus power for Rod AA at 0 - 100 MWD/MTU.

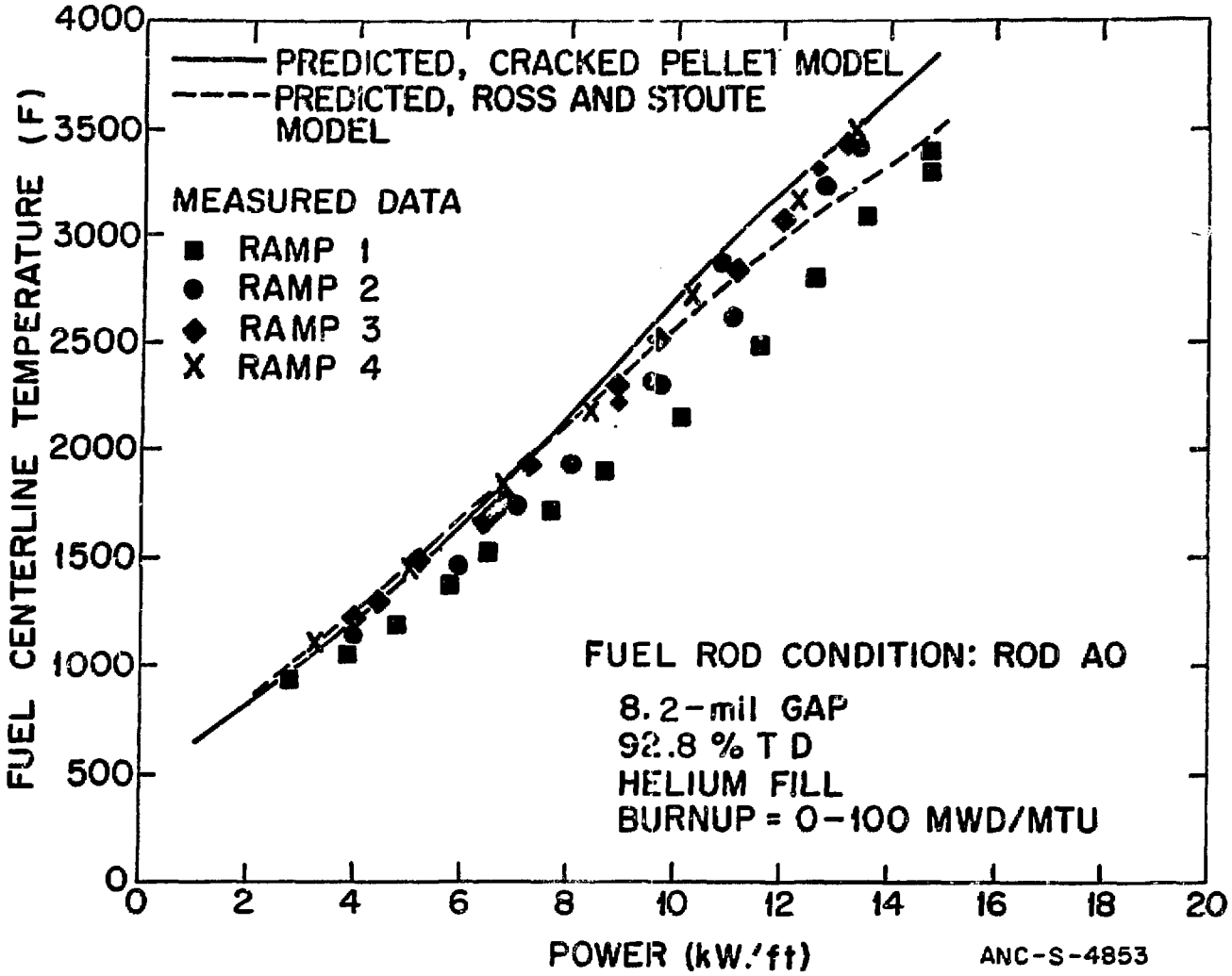

Figure 12 Measured and predicted fuel centerline temperature versus power for Rod AO at 0 - 100 MWD/MTU.

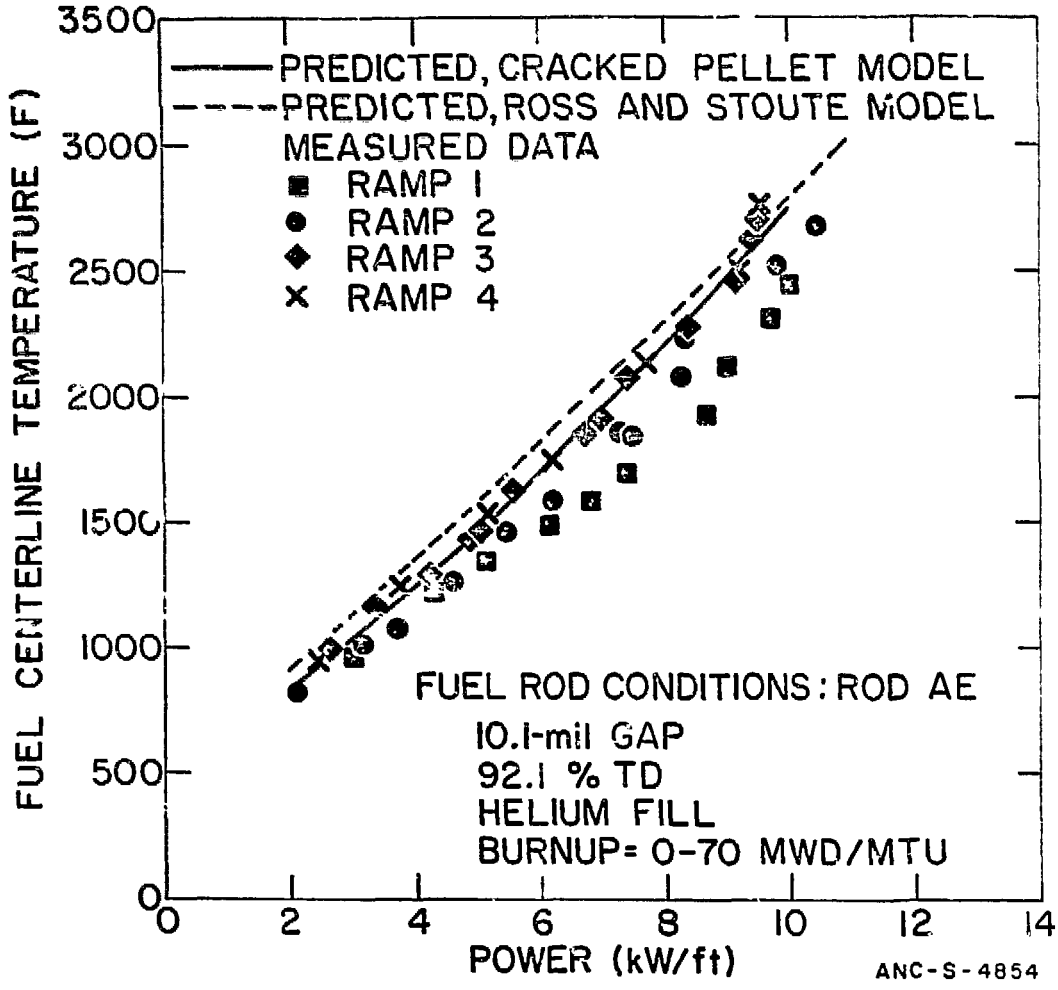

Figure 13 Measured and predicted fuel centerline temperature versus power for Rod AE at 0 - 70 MWD/MTU.

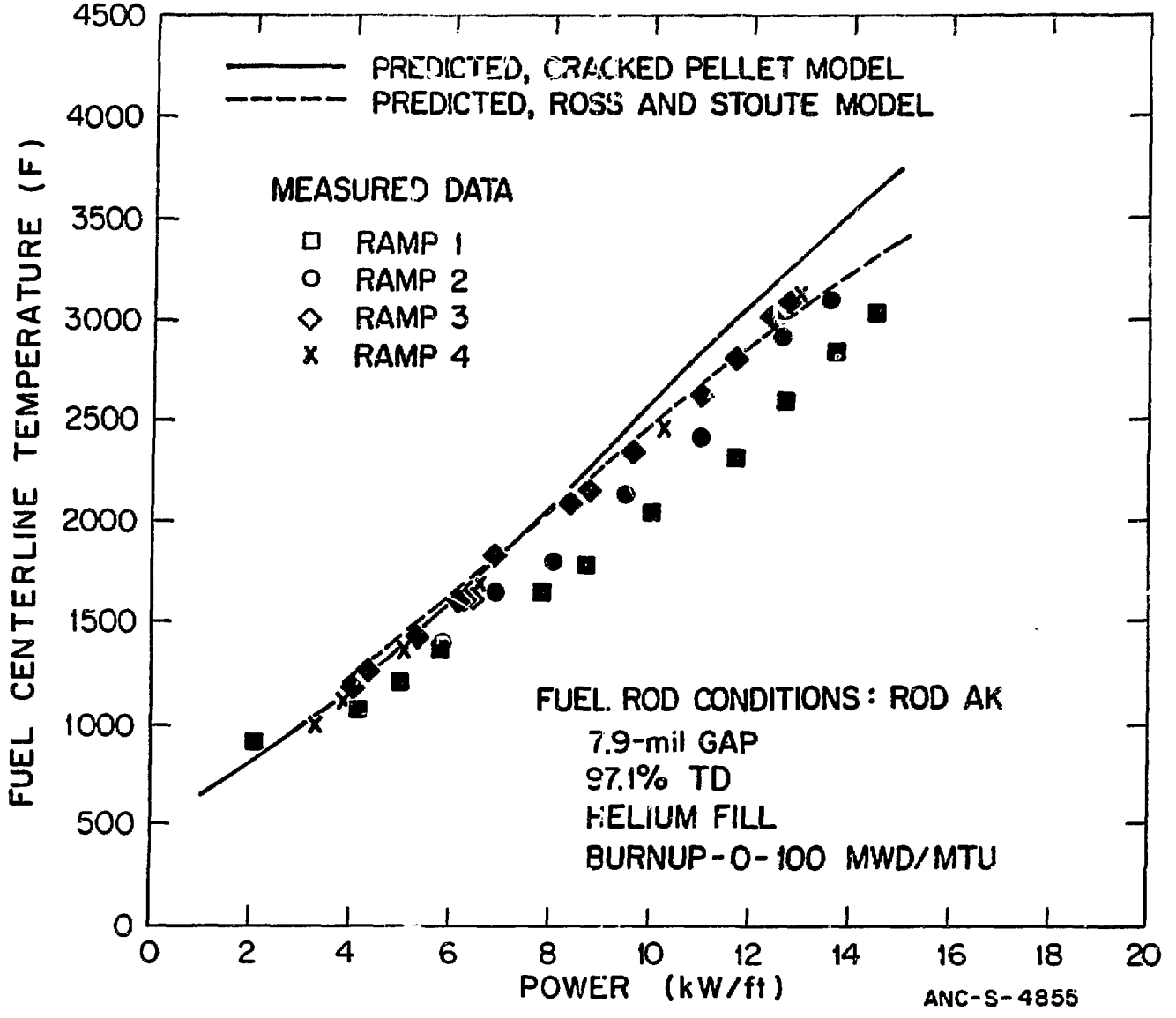

Figure 14 Measured and predicted fuel centerline temperature versus power for Rod AK at 0 - 100 MWD/MTU.

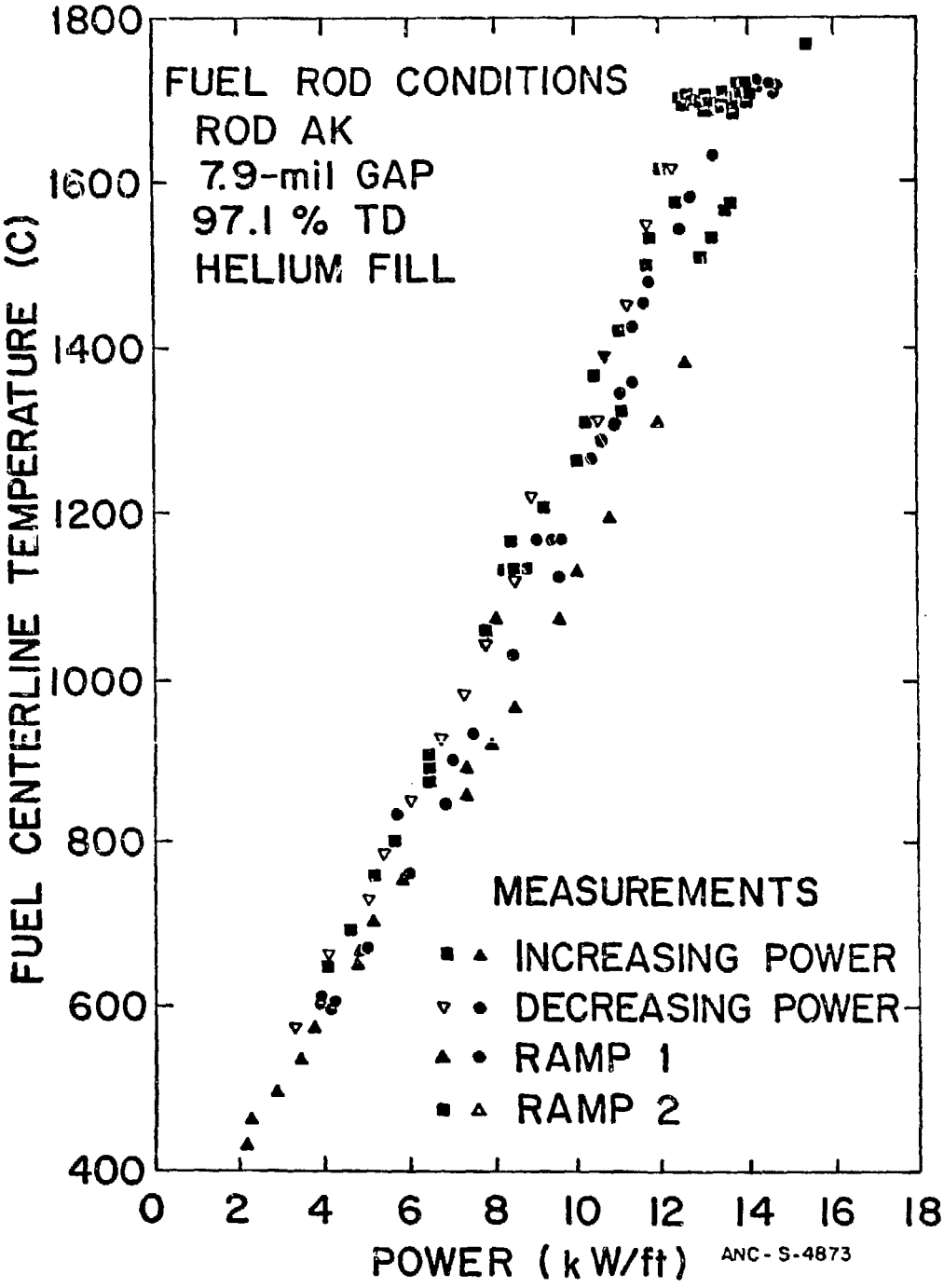

Figure 15 Measured fuel centerline temperature versus power for Rod AK during the first two power ramps.

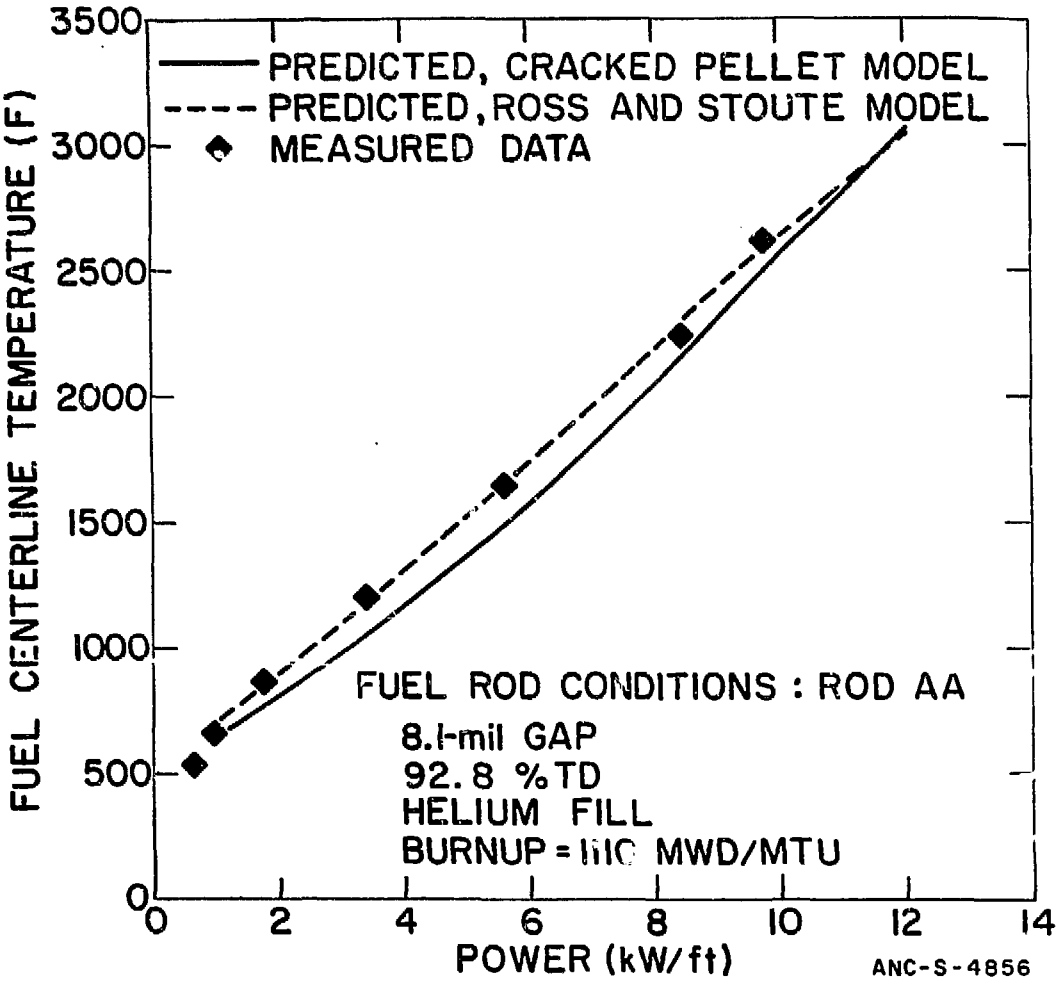

Figure 16 Measured and predicted fuel centerline temperature versus power for Rod AA at 1110 MWD/MTU.

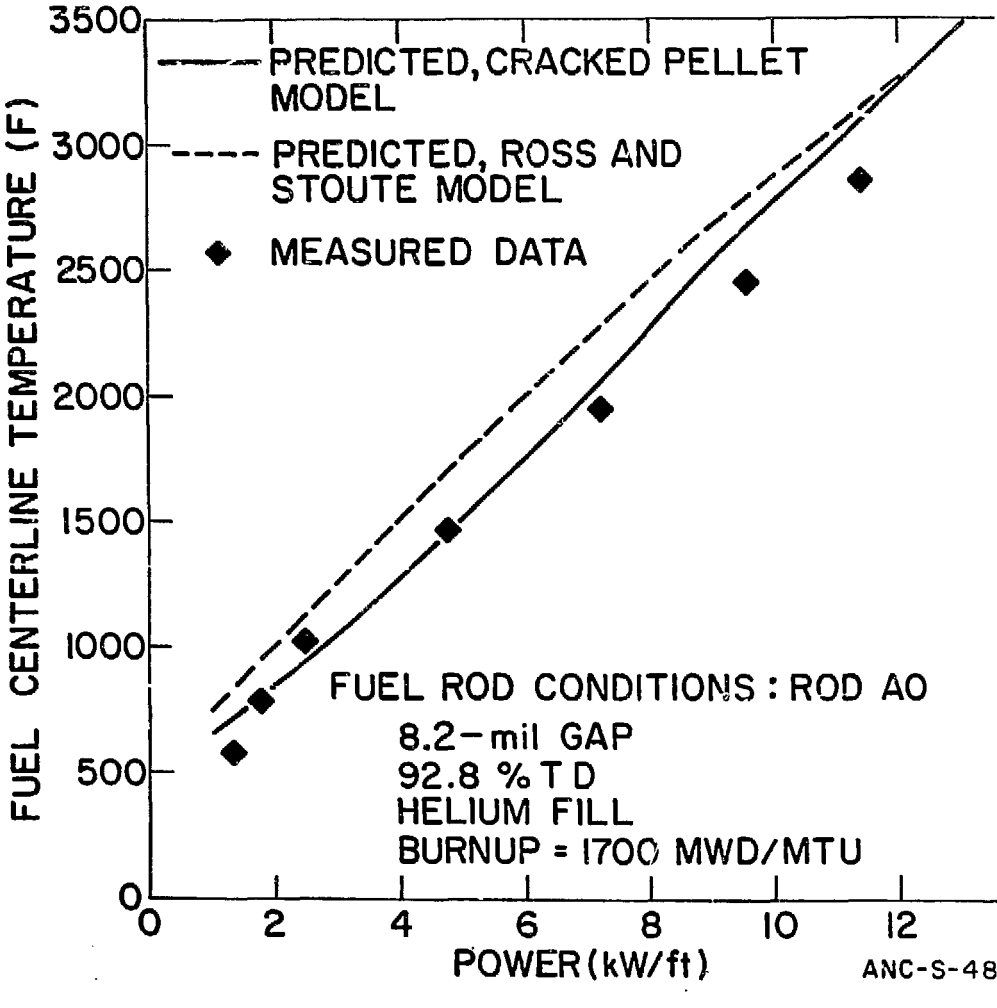

Figure 17 Measured and predicted fuel centerline temperature vers power for Rod AO at 1700 MWD/MTU.

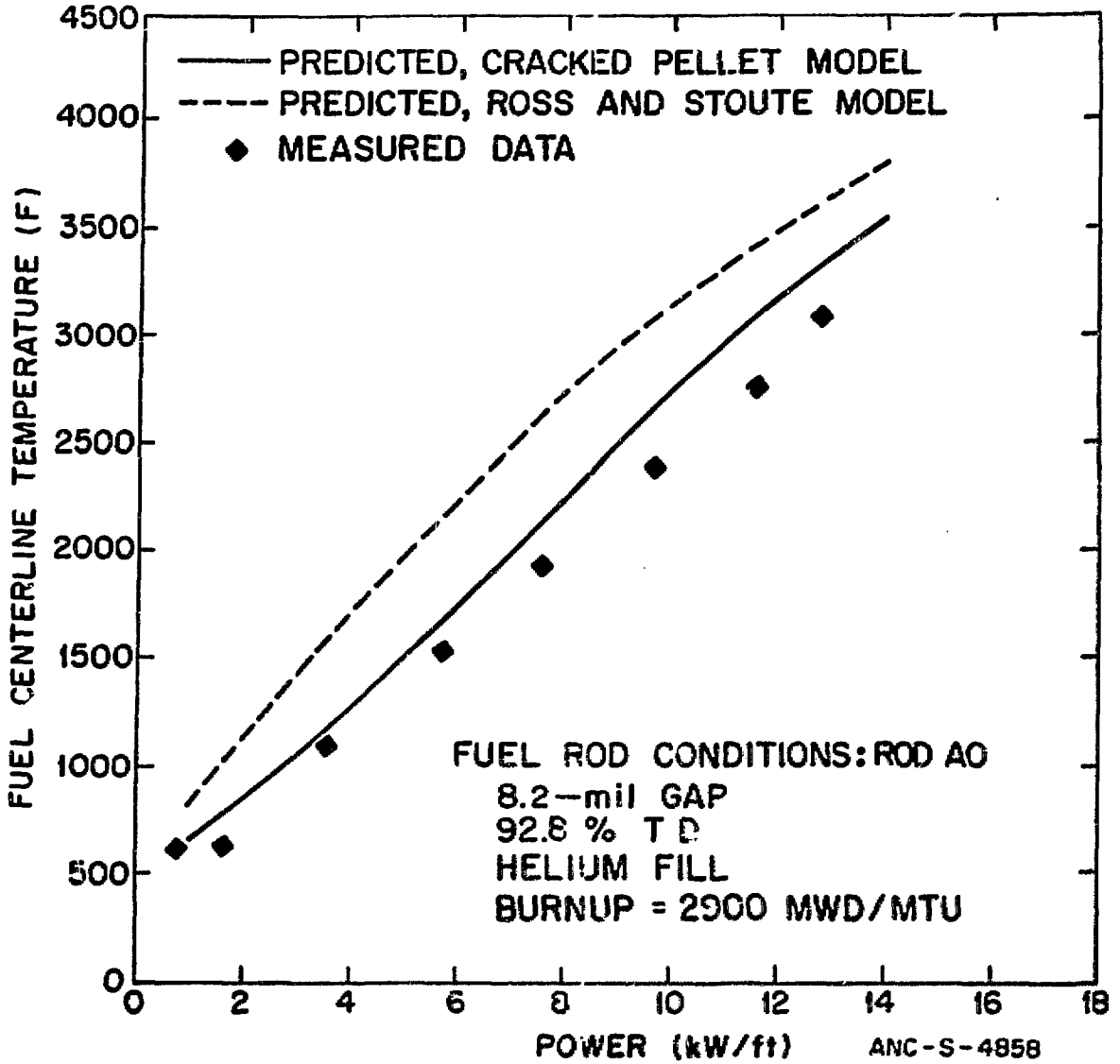

Figure 18 Measured and predicted fuel centerline temperature versus power for Rod A0 at 2900 MWD/MTU.

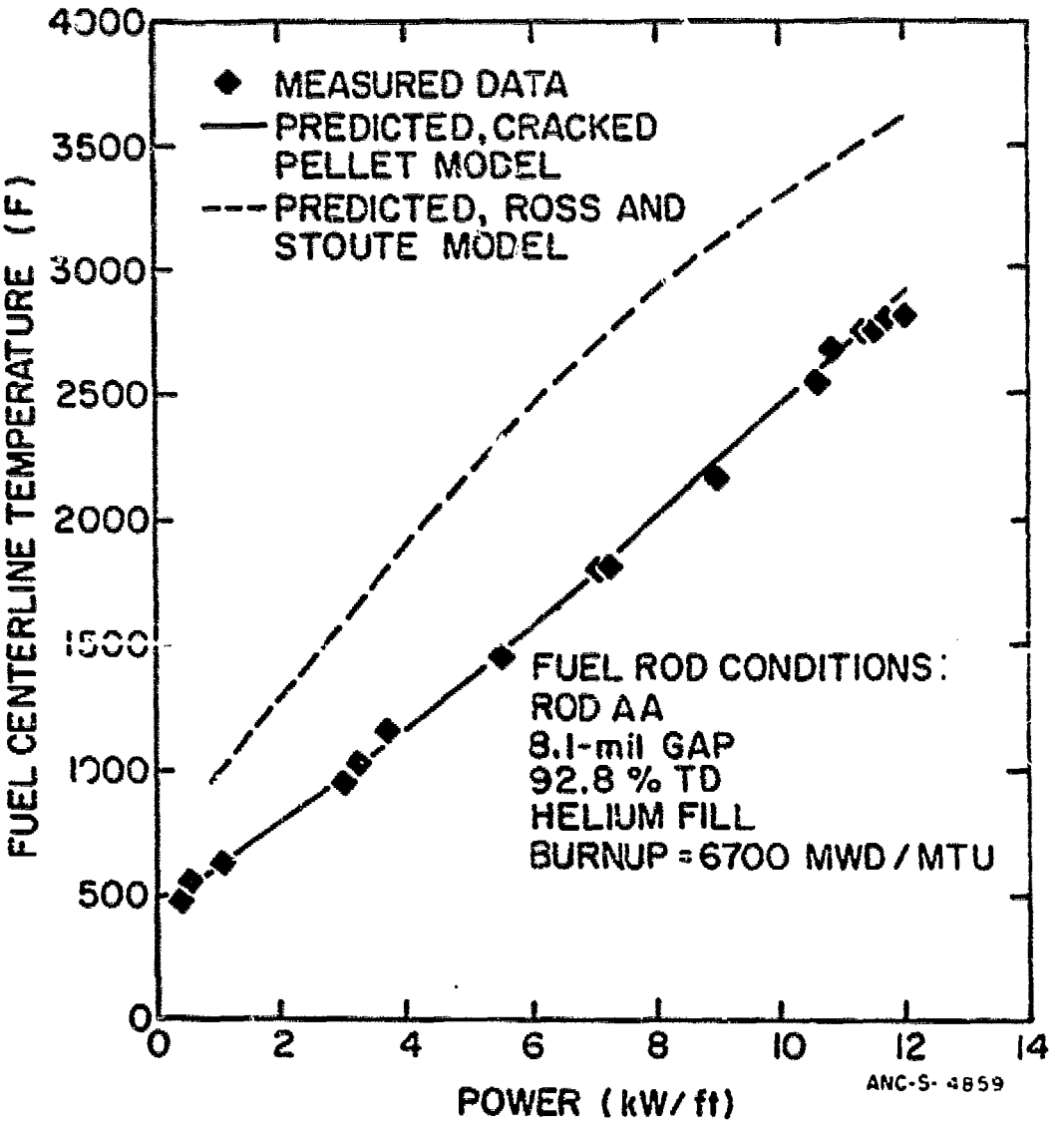

Figure 19 Measured and predicted fuel centerline temperature versus power for Rod AA at 6700 MWD/MTU.

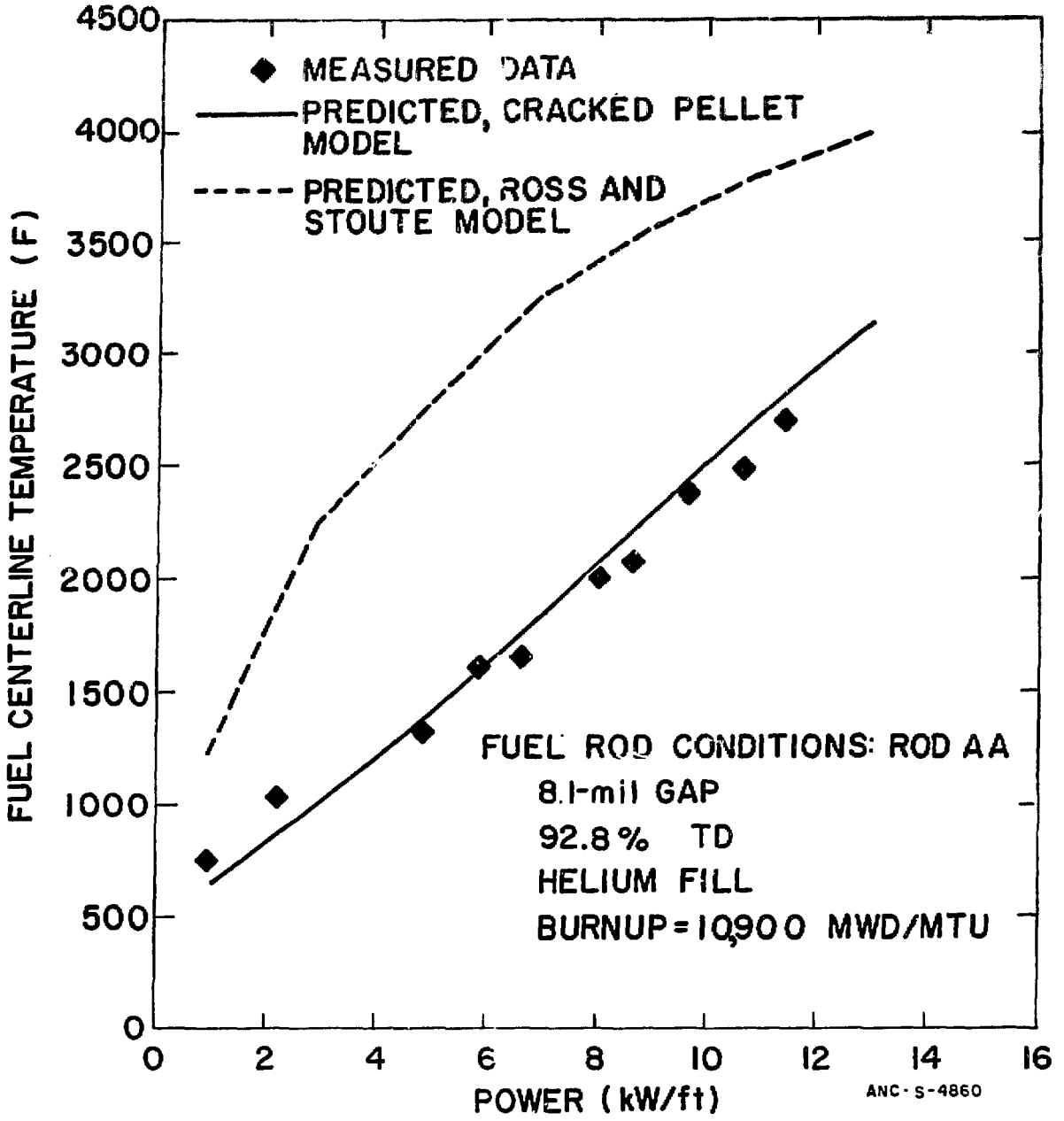

Figure 20 Measured and predicted fuel centerline temperature versus power for Rod AA at 10900 MWD/MTU.

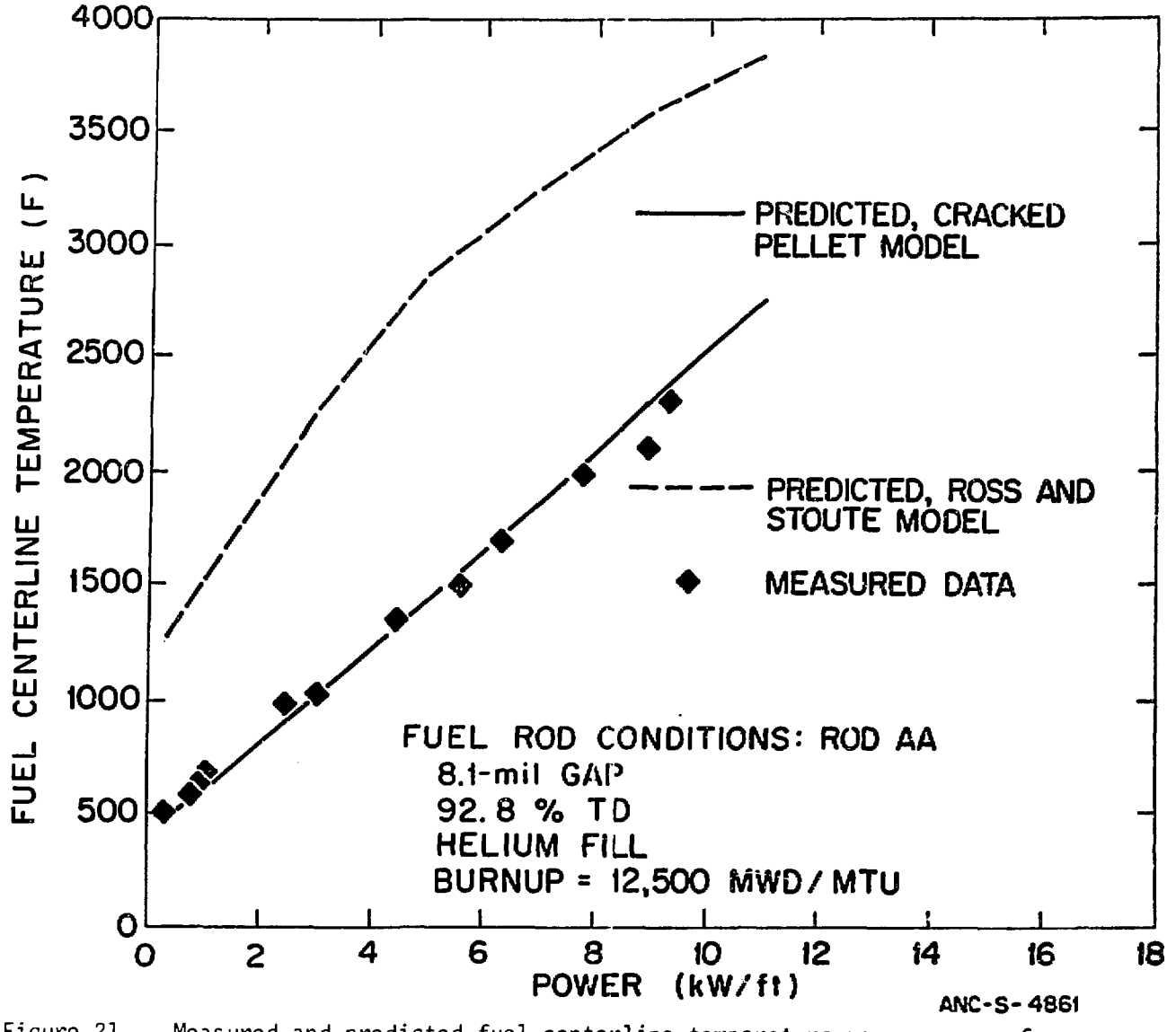

Figure 21 Measured and predicted fuel centerline temperature versus power for Rod AA at 12,500 MWD/MTU.

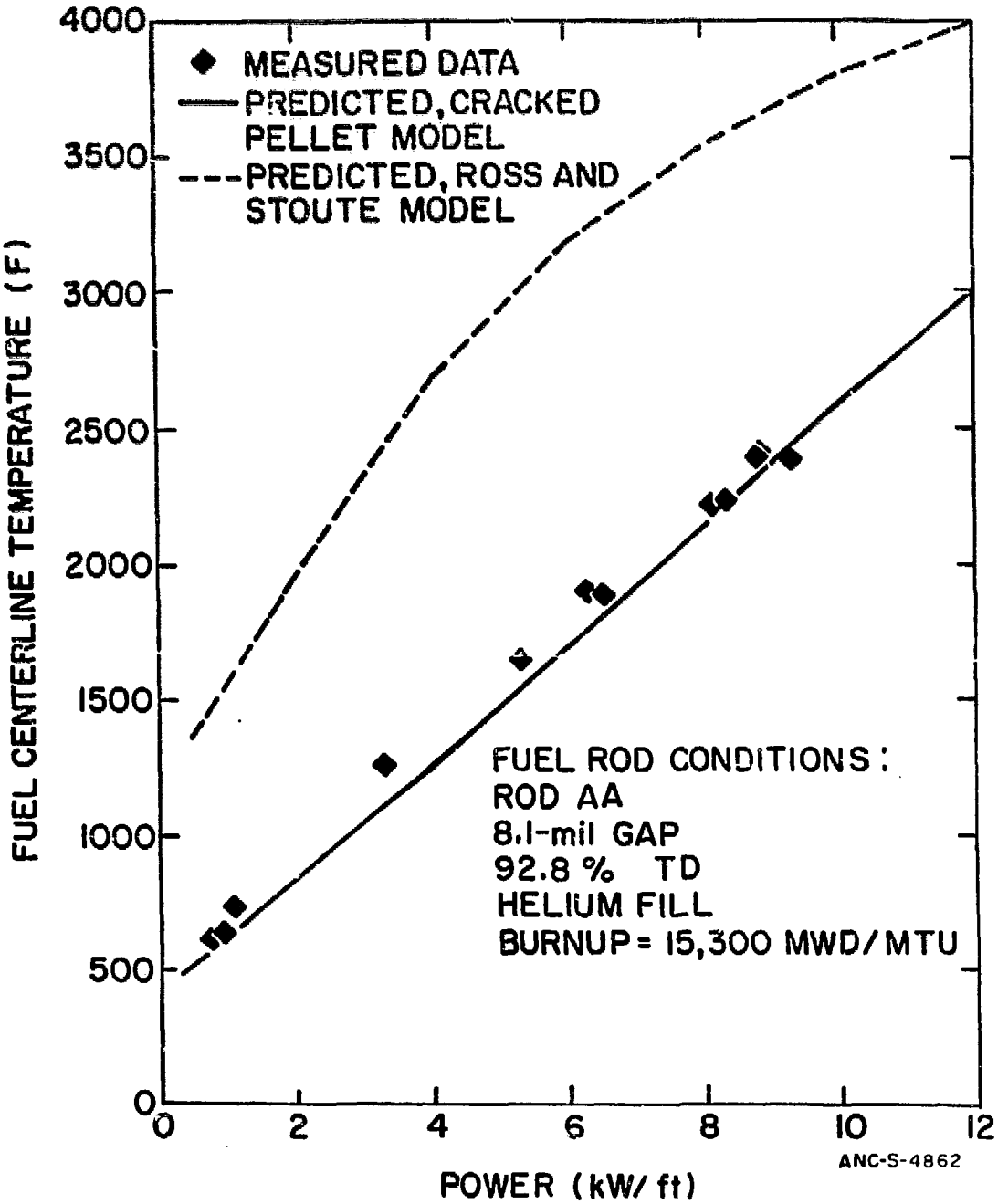

Figure 22 Measured and predicted fuel centerline temperature versus power for Rod AA at 15,300 MWD/MTU.

PROPOSED CRACKED PELLET GAP CONDUCTANCE MODEL

- PREVIOUSLY USED
  - OPEN GAP
    - ROSS AND STOUTE
    - CONDUCTION ACROSS THE GAP GAS AND RADIATION
    - CONCENTRIC GAS GAP
  - CLOSED GAP
    - LINEAR RELATIONSHIP BETWEEN CONTACT GAP CONDUCTANCE AND FUEL-CLADDING CONTACT PRESSURE
- PROPOSED MODEL
  - OPEN GAP
    - CONDUCTION THROUGH THE GAS IN THE OPEN GAP AND ZERO PRESSURE CONTACT CONDUCTANCE - PROPORTIONAL TO FRACTION OF FUEL-CLADDING CONTACT
    - CRACKED PELLET AND ECCENTRIC FUEL-CLADDING GEOMETRY MODELED
    - FRACTION OF FUEL-CLADDING CONTACT FUNCTION OF BURNUP AND THE RATIO OF HOT DIAMETRAL GAP TO PELLET DIAMETER
  - CLOSED GAP
    - NON LINEAR RELATIONSHIP BETWEEN CONTACT GAP CONDUCTANCE AND FUEL- CLADDING CONTACT PRESSURE
    - MODELS BOTH PLASTIC AND ELASTIC FLOW AT THE FUEL AND CLADDING CONTACT POINTS

PROPOSED CRACKED PELLET GAP CONDUCTANCE MODEL

GOVERNING EQUATIONS

- OPEN GAP

$$h_{gap} = (1-F)\,h_1 + F h_2$$

Where

$$F = \frac{1}{a_1\left[\frac{\Delta D \cdot 100}{D_F}\right]^{a_2} + a_3} + a_4$$

and

$$a_i = (a_{i_{EOL}} - a_{i_{BOL}})\left(1 - \frac{1}{\left[\frac{Bu-600}{1000}\right]^4 + 1}\right) + a_{i_{BOL}}$$

- CLOSED GAP

$$h_{gap} = C_1 P^n + \frac{k_{mix}}{\delta}$$

Where

$n = 1$ for $0 \leq P \leq 1000$ psi and $1/2$ for $P > 1000$ psi